



## An analysis of the mechanisms of North American pollutant transport to the central North Atlantic lower free troposphere

R. C. Owen,<sup>1</sup> O. R. Cooper,<sup>2</sup> A. Stohl,<sup>3</sup> and R. E. Honrath<sup>1</sup>

Received 6 January 2006; revised 10 April 2006; accepted 25 May 2006; published 26 August 2006.

[1] We use the FLEXPART Lagrangian particle dispersion model and observations from the PICO-NARE station to identify and analyze the transport of North American anthropogenic emissions to the central North Atlantic lower free troposphere (FT) during July 2003. FLEXPART adequately captured the occurrence of CO transport events, simulating all but 1 of the 16 observed events while producing only 3 events not observed. Low-level transport (below 3 km) was responsible for most events. Three case studies of this type are presented. Export from the North American boundary layer in these events was the result of eastward advection over the ocean or transport in a weak warm conveyor belt airflow. Once over the ocean, transport was governed by geostrophic winds between the Azores/Bermuda High (ABH) and transient northerly lows. The varying locations of the ABH and northerly lows determine the pathway of this type of event. As a result, other events similar to those analyzed here reach Europe. Transported below 3 km, these events were observed in the lower FT over the Azores and were accompanied by O<sub>3</sub> enhancements. Thus the lower marine FT may provide a transport environment significantly different from the marine boundary layer, where O<sub>3</sub> destruction is believed to dominate. In the fourth case study, North American emissions were lofted to 6–8 km in a warm conveyor belt, captured for 2 days in the midtropospheric circulation of the associated cyclone, and then entrained in the same cyclone's dry airstream and transported down to the Azores.

**Citation:** Owen, R. C., O. R. Cooper, A. Stohl, and R. E. Honrath (2006), An analysis of the mechanisms of North American pollutant transport to the central North Atlantic lower free troposphere, *J. Geophys. Res.*, *111*, D23S58, doi:10.1029/2006JD007062.

### 1. Introduction

[2] On the basis of extensive study over the past two decades, it is recognized that emissions exported from large urban/industrial regions like the eastern United States, Europe, and Asia have large-scale impacts on levels of O<sub>3</sub>, particles, and other species over downwind continents and in the remote atmosphere [e.g., Parrish *et al.*, 1998; Hoell *et al.*, 1997; Trickl *et al.*, 2003; Pochanart *et al.*, 2003; Jaffe *et al.*, 1999; Ryall *et al.*, 1998]. These impacts are important because of their effect on the ability of downwind nations to attain air quality standards [Li *et al.*, 2002; Park *et al.*, 2004], the important role of O<sub>3</sub> as a source of OH radical, and the roles of O<sub>3</sub> and particles in the Earth's energy budget [Houghton *et al.*, 2001].

[3] Most anthropogenic emissions occur at or near ground level over the continents. The details of the export of these emissions from the continental boundary layer af-

fect pollutant lifetimes and transformations downwind. For example, emissions transported to the marine boundary layer (MBL), where photochemical lifetimes are typically shorter, are less likely to exert a large-scale impact than are those exported to the free troposphere (FT). In contrast, emissions rapidly transported to the upper troposphere, where many loss processes are less effective and wind speeds are high, are more likely to have detectable large-scale impacts [Stohl *et al.*, 2002b], but may be less likely to directly affect downwind surface concentrations.

[4] Uplift in the warm conveyor belt (WCB) airstream ahead of cold fronts associated with midlatitude cyclones provides an effective mechanism for rapid transport to the middle and upper troposphere. Episodic WCB export associated with passing cyclones has been identified as a dominant mechanism for rapid transport of both North American and Asian emissions to the middle and upper troposphere [e.g., Stohl and Trickl, 2001; Cooper *et al.*, 2004]. The combination of rapid uplift and rapid transport in the upper troposphere results in impacts on middle to upper tropospheric composition well downwind, and significant enhancements of O<sub>3</sub>, CO, and nitrogen oxides over Europe resulting from WCB export of North American emissions have been documented [Stohl and Trickl, 1999; Trickl *et al.*, 2003; Auvray and Bey, 2005; Huntrieser *et al.*, 2005]. An alternative mechanism for even more rapid uplift

<sup>1</sup>Department of Civil and Environmental Engineering, Michigan Technological University, Houghton, Michigan, USA.

<sup>2</sup>Cooperative Institute for Research in Environmental Sciences, University of Colorado/NOAA Earth System Research Laboratory, Boulder, Colorado, USA.

<sup>3</sup>Norwegian Institute for Air Research, Kjeller, Norway.

of pollutants to the upper troposphere is provided by convection [Dickerson *et al.*, 1987], leading to significant impacts above the pollutant source region [e.g., Pickering *et al.*, 1990; Thompson *et al.*, 1994], although transport to distant regions may be less rapid [Li *et al.*, 2005].

[5] Export out of the continental boundary layer can also occur at low altitudes, either as the result of episodic ventilation in the post cold front, an airstream associated with passing midlatitude cyclones [Cooper *et al.*, 2002] or via advection in the mean winds, not associated with frontal passages [Li *et al.*, 2002]. Transport speeds in the lower troposphere are less than those in the upper troposphere. As a result, the time for dilution and photochemical transformations is greater, and enhancements in mixing ratios well downwind are expected to be smaller. Perhaps for this reason, lower tropospheric export events have received less attention than WCB export and convection. However, lower tropospheric export fluxes are significant. For example, Li *et al.* [2005] determined that more than one third of the CO exported from North America in July GOES-CHEM simulations occurred in the lowest 3 km. As noted above, the fate of emissions exported in these events is dependent, in part, on whether transport occurs in the MBL or FT. Although most of the lower 3 km column is within the daytime continental boundary layer, downwind transport is likely to occur in the lower FT as well as in the MBL. This is the result of the differing boundary layer structure over the ocean, relative to that over land. As discussed by Angevine *et al.* [2004], once exported continental air reaches the Atlantic Ocean, a statically stable near-surface layer develops, growing over time and isolating the polluted air mass from the ocean surface. Eventually, a steady state MBL must develop, but central North Atlantic MBL heights are much smaller than 3 km (e.g., typically less than 1 km during summer over the central and eastern North Atlantic [Rodríguez *et al.*, 2004]). For example, recent measurements have shown that polluted air containing relatively high levels of nitric acid (10s of ppb), can be transported hundreds of km downwind of source regions. These plumes were observed in layers as low as a few hundred meters altitude, decoupled from the surface and above the marine boundary layer [Neuman *et al.*, 2006].

[6] In order to study the photochemical evolution of North American emissions transported downwind in the lower FT, we established the 2.2-km-altitude PICO-NARE station in the Azores Islands in July 2001. Analyses of CO and O<sub>3</sub> measurements made there during the summers of 2001–2003 demonstrate that events of long-range transport in the lower FT occur and are detectable at this location, typically ~3–6 days downwind [Honrath *et al.*, 2004]. Here, we use these measurements in combination with simulations by the FLEXPART particle dispersion model [Stohl *et al.*, 1998] to identify events during which eastern North American emissions significantly impacted the central North Atlantic lower FT during July 2003. The focus of this paper is a descriptive analysis of the meteorological scenarios responsible for four representative events. Three of these originated as lower tropospheric export events and are expected to be typical of the events responsible for lower tropospheric pollution export from eastern North America. The fourth involves an interesting combi-

nation of uplift in a WCB followed by subsidence in the same cyclone's dry airstream.

## 2. Methods

### 2.1. PICO-NARE Station Measurements

[7] Measurements of CO, O<sub>3</sub>, and relative humidity (RH) made at the PICO-NARE station during July 2003 were used to identify periods apparently impacted by upwind emissions of CO and of O<sub>3</sub> precursors, and the CO measurements were used with FLEXPART simulations (described below) to identify periods of North American emission transport to the station.

[8] The PICO-NARE station is located on the summit of Pico mountain, an inactive volcano on Pico Island in the Azores, Portugal (38.47° north latitude, 28.4° west longitude). Station altitude (2.2 km) is well above the regional MBL, which is typically less than 1 km in height during summer. Upslope flow on Pico mountain is not frequent, even during summer, occurring on 39% of the days during a period of intensive meteorological measurements in summer 2004, and bringing MBL air to the summit on only a fraction of those days (J. Kleissl *et al.*, The occurrence of upslope flows at the Pico mountaintop observatory: A case study of orographic flows on a small, volcanic island, submitted to *Journal of Geophysical Research*, 2006). During July 2003, the period analyzed here, about one half of the days experienced the low synoptic winds and strong insolation necessary for upslope flow on Pico mountain. Of the events discussed in detail below, only the last 3 hours of event 4 are potentially affected by buoyant upslope flow. However, relative humidity remained below 50% during that period, indicating a lack of significant MBL impact.

[9] Carbon monoxide was determined using a modified commercial nondispersive infrared absorption instrument (Thermo Environmental, Inc., Model 48C-TL), calibrated daily with standards referenced to the NOAA CMDL standard. Ozone was obtained with two commercial ultraviolet absorption instruments (Thermo Environmental Instruments Inc., Franklin, Massachusetts; Model 49C). On the basis of comparisons between these instruments and a NOAA CMDL network ozone standard conducted in 2001 and 2004 and between the two instruments in 2003 and 2004, the raw measurements from the first instrument (used prior to 19 July) were reduced by 0.2%, while those from the second instrument (used after 19 July) were increased by 2.6%. The resulting O<sub>3</sub> mixing ratios are 5 to 7% lower than those reported previously [Honrath *et al.*, 2004], as a result of the additional intercomparisons now available. The 30-min average CO measurements used here have 2- $\sigma$  precision of  $\pm 3$  ppbv or better; accuracy is  $\pm 6\%$ . For O<sub>3</sub>, precision is 1 ppbv or better, and accuracy is estimated as  $\pm 3\%$ , the maximum adjustment applied to the July 2003 raw O<sub>3</sub> measurements.

[10] The July 2003 CO and O<sub>3</sub> measurements have been presented previously [Honrath *et al.*, 2004]. Further details on the PICO-NARE station, the measurements made there, and the frequency of upslope flow to the station are provided elsewhere [Honrath *et al.*, 2004].

### 2.2. FLEXPART

[11] We used the FLEXPART (version 5.1) particle dispersion model [Stohl *et al.*, 1998; Stohl and Thomson, 1999]

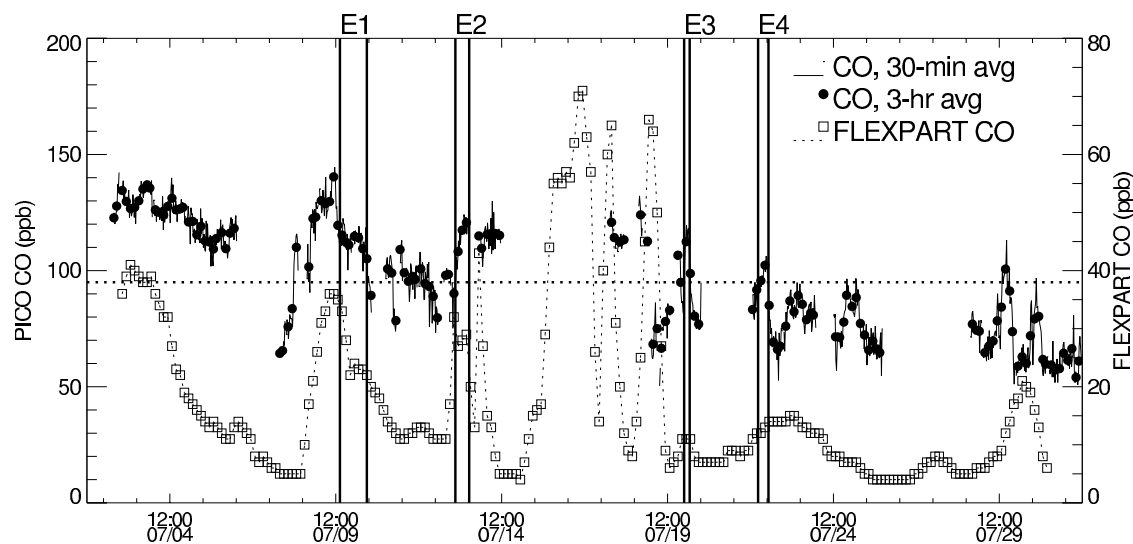


**Figure 1.** Time series of 30-min (solid line) and 3-hour averaged (solid circles) CO measured at the PICO-NARE station and CO from FLEXPART retroplumes (open boxes and dotted line) initialized over a 3-hour period. The case study events discussed in the text are marked with solid vertical lines.

to simulate CO enhancements at the PICO-NARE station resulting from the transport of North American emissions. Forward simulations were used for visualizing the advection and dispersion of CO due to the synoptic scenario. Backward simulations, which produce a cloud of particles that is traced backward in time (termed a retroplume) were primarily used in the same manner as backward trajectories: to trace the flow of air, helping to identify important source regions. However, a major advantage over simple backward trajectories is that they can be used to calculate a time series of the contribution of North American CO to the total CO at the station by multiplying the residence times of retroplume particles in the lowest 300 m over North America, a measure of the sensitivity to emission input, by the emissions flux at each location, as described by *Seibert and Frank* [2004] and used in previous studies [*Stohl et al.*, 2003; *Huntrieser et al.*, 2005]. Simulations were conducted for the month of July 2003.

[12] FLEXPART was driven with data from the European Centre for Medium Range Weather Forecasts (ECMWF) [European Center for Medium-Range Weather Forecasts, 1995] with  $1^\circ$  horizontal resolution, 60 vertical levels and a temporal resolution of 3 hours, using meteorological analyses at 0000, 0600, 1200, and 1800 UTC, and ECMWF 3-hour forecasts initialized at these times. It has been found that the use of analyzed fields can result in an overestimation of mixing between air masses [*Stohl et al.*, 2004]. While forecast fields do not experience this overestimation, they will drift away from the real meteorological situation and so the use of analyzed fields is a necessity for any simulation beyond a few hours. In general, the backward simulations show that our events have a fairly coherent meteorological situation and exhibit relatively little mixing between the source and the station. Therefore we do not believe this effect is significant enough to change the conclusions of this paper.

[13] In the forward mode, CO emissions were released into the lowest 150 m of the atmosphere over North America. CO emissions were based on the EDGAR version

3.2 inventory [*Olivier and Berdowski*, 2001], which uses 1995 as the base year and has a  $1^\circ$  resolution. A total of 11 million particles were released per 20 days over North America with particles released over 3-hour intervals. The number of particles released into each grid cell was determined by scaling the total number of particles released by the emissions in each grid cell. Particles were dropped from the simulation after 20 days and were conserved up to that time. Thus the simulations model only CO enhancements caused by North American emissions over the previous 20 days.

[14] Retroplumes were initiated every 3 hours with 25,000 particles released over a 3-hour time interval into a  $1^\circ \times 1^\circ$  grid box centered on the PICO-NARE station, over an altitude range of 1750 m asl to 2750 m asl. Retroplume simulations were run for 20 days backward in time. To calculate CO mixing ratios at the PICO-NARE station resulting from North American emissions, the same EDGAR emission inventory was used with the retroplume results, using the method of *Seibert and Frank* [2004]. No attempt was made to adjust the emission inventory for the CO emissions reductions that have occurred since 1995 [*Parrish et al.*, 2002], as moderate biases in the FLEXPART-predicted mixing ratios would not affect our interpretation.

### 2.3. Event Selection

[15] Only periods with observed CO above 95 ppbv during the study period of July 2003 were identified as potentially impacted by North American outflow. This cutoff value was selected as the approximate dividing point between apparent background observations and enhanced CO observations in the summer 2003 PICO-NARE measurements [*Honrath et al.*, 2004]. These periods of elevated CO were then further subdivided on the basis of evidence of changes in flow pathways, as indicated by the FLEXPART retroplumes, and apparent changes in air masses, as indicated by correlated changes in the CO and  $O_3$  mixing ratios and relative humidity. For example, the period from 1900

**Table 1.** Events of Elevated CO Observations During July 2003<sup>a</sup>

Event	Start Time <sup>b</sup>	End Time <sup>b</sup>	Observed CO <sup>c</sup>	Observed O <sub>3</sub> <sup>c</sup>	N. American CO <sup>d</sup>	Transport Time <sup>e</sup>	Transport Height <sup>e</sup>
a	1900 2 Jul	2230 4 Jul	129 ppb	48 ppb	34 ppb	5–7 days	2–4 km
b	2300 4 Jul	1230 6 Jul	116 ppb	N/A	14 ppb	5.5 days	2–4 km
c	0600 8 Jul	0900 8 Jul	109 ppb	N/A	6 ppb	N/A	N/A
d	1530 8 Jul	1700 8 Jul	101 ppb	N/A	15 ppb	4.5 days	3–4 km
e	1800 7 Jul	1500 9 Jul	128 ppb	N/A	31 ppb	4.5 days	2–5 km
f: 1	1530 9 Jul	1030 10 Jul	113 ppb	N/A	25 ppb	5 days	2–6 km
g	0030 11 Jul	0530 11 Jul	102 ppb	N/A	15 ppb	6 days	2–6 km
h	1100 11 Jul	0730 12 Jul	101 ppb	30 ppb	14 ppb	5 days	2–4 km
i	1900 12 Jul	2300 12 Jul	98 ppb	28 ppb	15 ppb	5 days	2–3 km
j: 2	0300 13 Jul	1230 13 Jul	114 ppb	56 ppb	30 ppb	4.5 days	2–7 km
k	2000 13 Jul	1130 14 Jul	114 ppb	68 ppb	22 ppb	5.5 days	2–8 km
l	1800 17 Jul	0430 18 Jul	115 ppb	N/A	45 ppb	7 days	2–4 km
m	1530 18 Jul	1800 18 Jul	124 ppb	N/A	14 ppb	5 days	2–4 km
n: 3	0030 20 Jul	0400 20 Jul	113 ppb	50 ppb	11 ppb	5 days	2 km
o: 4	0600 22 Jul	1300 22 Jul	100 ppb	51 ppb	15 ppb	7 days	2 km
p	1430 29 Jul	1930 29 Jul	101 ppb	49 ppb	14 ppb	5 days	2 km

<sup>a</sup>NA, not available.

<sup>b</sup>Times are in UTC, which is approximately 2 hours later than local solar time.

<sup>c</sup>Mean mixing ratios observed during the indicated periods.

<sup>d</sup>Mean North American contribution to observed CO, calculated using FLEXPART as described in the text.

<sup>e</sup>Travel time and approximate altitude of FLEXPART retroplume particles released during the event that reached eastern North America.

UTC on 2 July to 1230 UTC on 6 July was identified as potentially affected by North American outflow, as CO levels were well above the 95 ppb cutoff. However, this period was divided into two events based off an abrupt change in CO levels (Figure 1) and a change in the flow path indicated by the FLEXPART retroplumes (not shown).

### 3. Results

[16] CO measurements and FLEXPART-simulated North American CO at the PICO-NARE station during the July 2003 study period are shown in Figure 1. The 16 events selected as described above are summarized in Table 1. These 16 events account for 52% of the 416 CO measurement hours during the study period. Mean observed CO and O<sub>3</sub> levels during each event may be compared to the most common CO level observed at the PICO-NARE station during apparent background periods in summer 2003, approximately 80 ppb (the “low-CO mode” [Honrath *et al.*, 2004]), and to the median O<sub>3</sub> mixing ratio during periods when CO was below 80 ppbv, 24 ppbv.

[17] Also shown in Table 1 are three columns based on the FLEXPART simulations: the mean North American contribution to the CO mixing ratio calculated using FLEXPART during each event, and the travel time and transport height between the responsible source region and the station. Travel times were estimated using 24-hour-average retroplume locations. Transport heights were estimated using retroplume clusters. (More precise information on transport heights is provided for the four case studies below.) The North American CO contributions summarized in Table 1 average 20 ppbv, and contributions of at least 10 ppbv are simulated during all events but one. Importantly, the events listed in Table 1, which were actually detected at the PICO-NARE station, account for all but four of the periods when FLEXPART-simulated North American CO contributions exceeded 10 ppbv. Of the four FLEXPART events not detected in the measurements, one was the result of biomass-burning emissions present in the EDGAR emission inventory in a region of Canada with no active fires

during July 2003, and two had only moderate FLEXPART CO enhancements of less than 15 ppbv. This high degree of consistency between CO events simulated by FLEXPART and those detected at the PICO-NARE station indicates that FLEXPART is adequately simulating the transport responsible for North American pollution transport to the PICO-NARE station.

[18] The events listed in Table 1 include each of the July 2003 events identified in our previous analysis [Honrath *et al.*, 2004], in which events were identified solely on the basis of the occurrence of CO levels above 114 ppbv. However, some of these events have been further subdivided here on the basis of changes in flow, and Table 1 includes three additional events on 11–12 July as a result of the reduced CO cutoff used here. Our previous analysis identified North American anthropogenic emissions as a probable contributor to the enhanced CO observations during each of the July 2003 events also identified here, but also noted potentially significant impacts from biomass-burning emissions during several: from Siberian fires during events a–b and from fires in the western United States during events c–n. Our analysis here focuses on the transport of anthropogenic emissions, but is not inconsistent with the occurrence of upwind biomass-burning emissions.

[19] On the basis of a preliminary analysis of the events shown in Table 1, we selected for detailed analysis four periods for which the mechanisms of export from North America and transport to the Azores were relatively clear and that appeared to be representative of the events during the study period. These four events are numbered in Table 1 and indicated in Figure 1.

[20] The remainder of this section provides a descriptive analysis of each of these four events. The presentation of each event is divided into two parts: the export of emissions out of the North American boundary layer, including relevant aspects of the preceding meteorological situation, and the subsequent transport to the PICO-NARE station. This discussion makes use of the FLEXPART forward and retroplume simulations, GOES-EAST and METEOSAT infrared satellite images, and sea-level pressure from NOAA

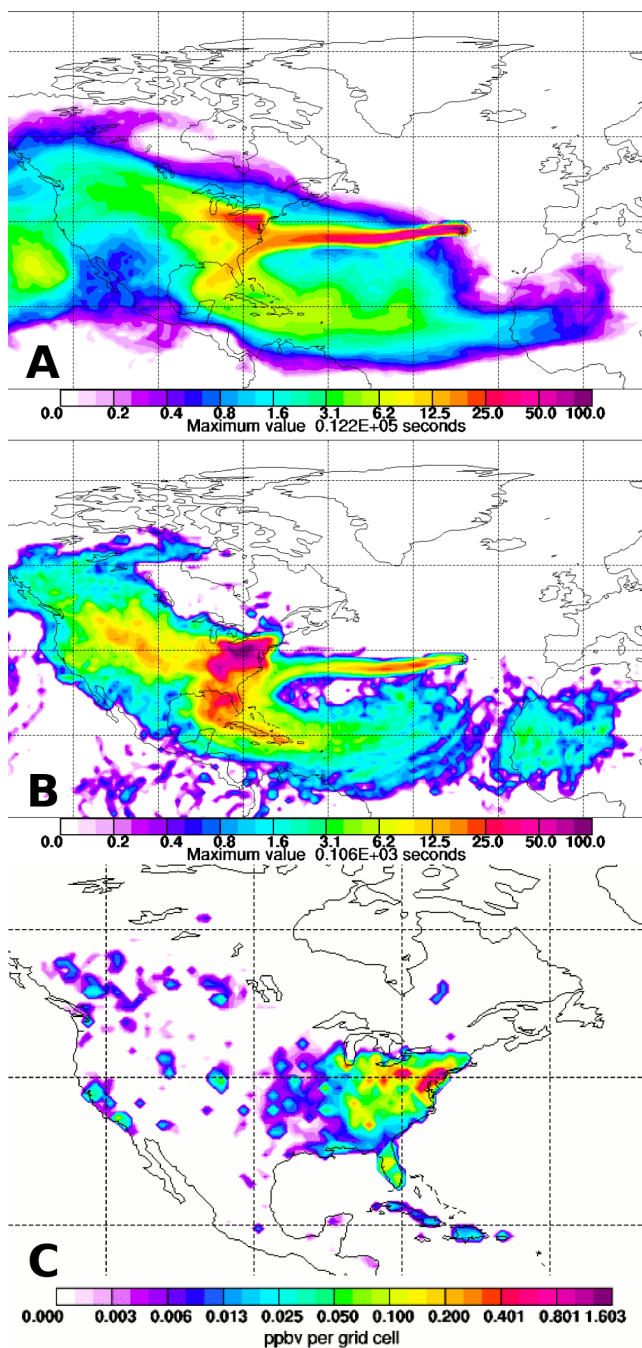


**Figure 2.** FLEXPART retroplume results for event 1. (a) Column integrated residence time, (b) residence time in the 0–300 m footprint layer, and (c) source contributions to CO mixing ratio calculated during this event. The retroplume was initiated from 0000–0300 UTC on 10 July.

NCEP Aviation Model analyses, which are presented in plots described in detail in the following section.

### 3.1. Event 1: Direct Transport From North America Associated With the Decaying Tropical Storm Bill

[21] The results of the FLEXPART retroplume simulation initialized during event 1 (0000–0300 UTC 10 July) are displayed in Figure 2. Figure 2 is divided into three parts.

Figure 2a shows the column-integrated residence time of retroplume particles. Plots of this type are most useful for identifying the overall horizontal transport pathway during the event. Figure 2b shows the residence time of retroplume particles in the lowest 300 m, termed the footprint layer. Footprint layer plots are most useful for identifying regions in which ground-level sources have the potential to influence pollutant levels during the event. Finally, Figure 2c shows the product of the footprint layer residence time and the CO emission inventory. This is the contribution of sources in each grid cell to the FLEXPART-calculated North American CO at the PICO-NARE station during this event. The color scales in Figures 2a and 2b are scaled to the maximum residence time, which is indicated below the color scale. For Figure 2c, the color scale indicates the mixing ratio contribution of each grid cell, in units of ppbv.

[22] The overall transport pathway during event 1 is apparent in Figure 2a, which indicates a coherent retroplume back to the U.S. east coast. (The blue colors surrounding the red, straight path result from recirculation, not direct transport.) Figure 2b shows that the plume resided in the footprint layer primarily over the heavily populated regions in the eastern United States, with smaller footprint residence times covering most of North America, the Atlantic south of the Azores and east of the United States, and western Africa. Figure 2c confirms that the majority of the FLEXPART-simulated CO came from the northeastern United States.

[23] Results from the retroplume simulation are presented in a second way in Figures 3a, 3c, 3e, and 3g. These figures show the location of retroplume particles on a single day, overlain on sea-level pressure isobars and infrared GOES-EAST and METEOSAT images. These plots indicate that the air sampled during this event was over the region with the highest CO contribution on 3 July (Figure 3a) and 4 July (Figure 3c), 6–7 days prior to arrival at the station.

[24] Figures 3b, 3d, 3f, and 3h show the results of the forward FLEXPART simulations, overplotted on the same infrared images, but this time in color, with reds and yellows indicating colder higher altitude cloud tops, and greens and dark blue indicating midlevel clouds and the Earth’s surface, respectively. Isolines of North American CO columns integrated over 0–3 km ( $\text{mg}/\text{m}^2$ ) are plotted over infrared images. These plots are useful for putting the events detected at the PICO-NARE station into the context of low-level CO export from North America. These images are discussed further below.

#### 3.1.1. Export Out of the U.S. Boundary Layer in a Low-Pressure System

[25] The meteorological situation that led to the export for this event began on 1 July, 9 days prior to its arrival at the PICO-NARE station, when tropical storm Bill made landfall over southern Mississippi. The low-pressure system associated with the storm was relatively weak, with a core sea level pressure of 998 hPa at 0000 UTC on 1 July. From 1 to 3 July the cyclone weakened, reaching 1009 hPa at 0000 UTC on 3 July, as it tracked northeast over the southeastern United States, reaching the Mid-Atlantic states on 3 July (–7 days).

[26] During these 3 days, a general region of high pressure persisted over the eastern United States and Atlantic ocean. The high over the United States dampened

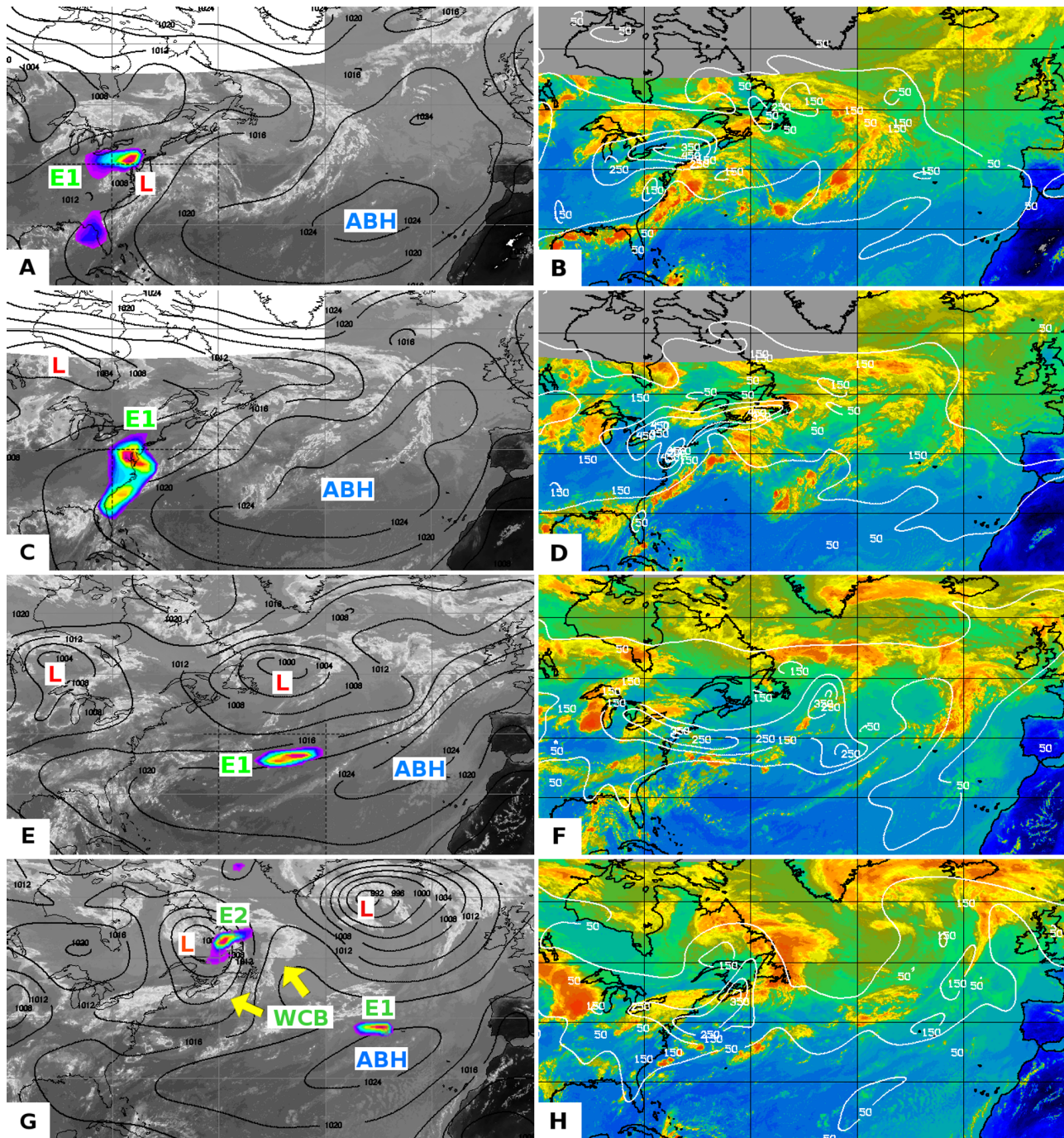


**Figure 3.** The 24-hour average location of the retroplume for event 1, plotted on top of combined GOES-EAST and METEOSAT infrared image and sea level isobars (left column) and 0–3 km CO column isolines (right column) plotted on top of the same infrared image shown in false color. The retroplume shown in the left column was initialized during event 1 (0000–0300 UTC 10 July). Times shown are (a and b) 1200 UTC 3 July, (c and d) 1200 UTC 4 July, (e and f) 1200 UTC 7 July, and (g and h) 1200 UTC 9 July. Labels on the left-hand plots indicate the retroplume for event 1 (E1) and pertinent meteorological features (low pressure centers, L; associated warm conveyor belts, WCB; and the Azores-Bermuda High, ABH). The event 2 retroplume (E2) is also indicated in Figure 3g.

convection in regions not affected by the decaying tropical storm. The high pressure over the Atlantic formed the western edge of the Azores-Bermuda High (ABH); its presence reduced the zonal export of pollution out of the region. As the low tracked northeast, the high over the

United States diminished, though strong convection was still limited to the regions of the decaying storm. By 3 July, the high over the United States had dissipated, leaving only the ABH off shore (Figure 3a), where it continued to prevent significant zonal pollution transport (Figure 3b).

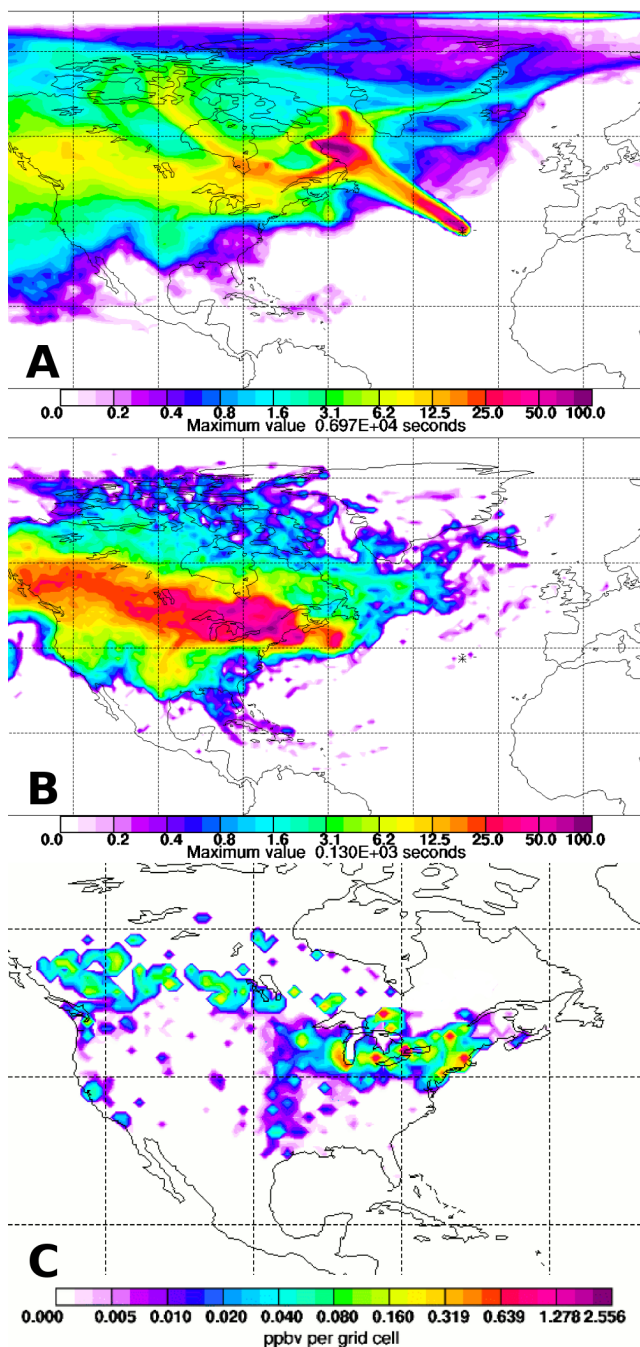


**Figure 4.** FLEXPART retriplume results for event 2. (a) Column integrated residence time, (b) residence time in the 0–300 m footprint layer, and (c) source contributions to CO mixing ratio calculated during this event. The retriplume was initiated from 1200–1500 UTC on 13 July.

[27] Between 1200 UTC on 3 July and 0000 UTC on 4 July, the low remained situated over Maryland and Delaware. It then tracked north, reaching Massachusetts by 1200 UTC on 4 July (–6 days, Figure 3c) This is the region where export of pollution had been dampened during the previous 3 days.

[28] During the first half of 4 July, a region of elevated CO developed in the area of the low. The region of intense

CO over southern New England is visible in the forward FLEXPART simulation, with column densities exceeding  $500 \text{ mg/m}^2$  for the 0–3 km column (Figure 3d). (The total column had only slightly higher maximum column densities in the region of high CO:  $550 \text{ mg/m}^2$ , not shown.)

[29] Early on 4 July, a new low-pressure system began to develop over northeastern Canada. As the low tracked east toward the Canadian east coast, the northwestern edge of the ABH began to retreat. This allowed increased zonal transport and, by 5 July, the column of pollution moved off shore, with the plume located about midway between the ABH and the Canadian low.

### 3.1.2. Transport to the Station Within Geostrophic Winds

[30] From 5 July (–5 days) to 7 July (–3 days), as the low tracked eastward over and across the Atlantic (Figure 3e), the plume also tracked eastward in the geostrophic wind between the ABH and the low. A large, coherent airstream, or river of CO is clearly visible in the forward FLEXPART results on 7 July (–3 days) as North American emissions were channeled out of the U.S. boundary layer through the two pressure features, with the portion of the plume for this event at the leading edge of the river of CO (Figure 3f).

[31] On 7 July, the low intensified, and by 8 July (–2 days) it had begun to track northeast. As the low moved northeast, away from the Azores, the ABH expanded northwest into the region west of the low. The retreat of the low to the northeast and the advance of the ABH to the northwest left the plume situated close to the center of the ABH early on 9 July (–1 day) (Figures 3g and 3h). During the last day of travel, the plume experienced slower transport than during the previous 4 days, but continued eastward to the Azores in the relatively weak westerly winds near the northern edge of the ABH, arriving at the PICO-NARE station while it was near the center of the ABH.

[32] In summary, the elevated CO levels observed at the Azores during this event were the result of a series of events beginning with an accumulation of pollution emissions over the eastern United States caused by a stagnant high-pressure system. The high over the United States diminished as a weak low (the result of a decaying tropical storm) moved into the region, and the accumulated emissions were mixed through the boundary layer near the center of the low. The pollution was then transported offshore in a weak westerly wind, and then to the PICO-NARE station in the geostrophic wind between the ABH and the low to the north. The path of transport was governed by the relative location of the ABH and the transient northern low. The CO enhancement sampled at the PICO-NARE station during this event was the result of the southern edge of a river of CO, which was channeled across the Atlantic between the ABH and the northern low (Figures 3g and 3h).

## 3.2. Event 2: Lofting and Subsidence Associated With a Midlatitude Cyclone

[33] The retriplume pathway for this event, shown in Figure 4a, differs significantly from that of event 1. The air sampled during this event traveled directly from the northeastern Canadian coast, but originated in the footprint layer (0–300 m) over the northern United States and southern Canada (Figure 4b). The FLEXPART-simulated North

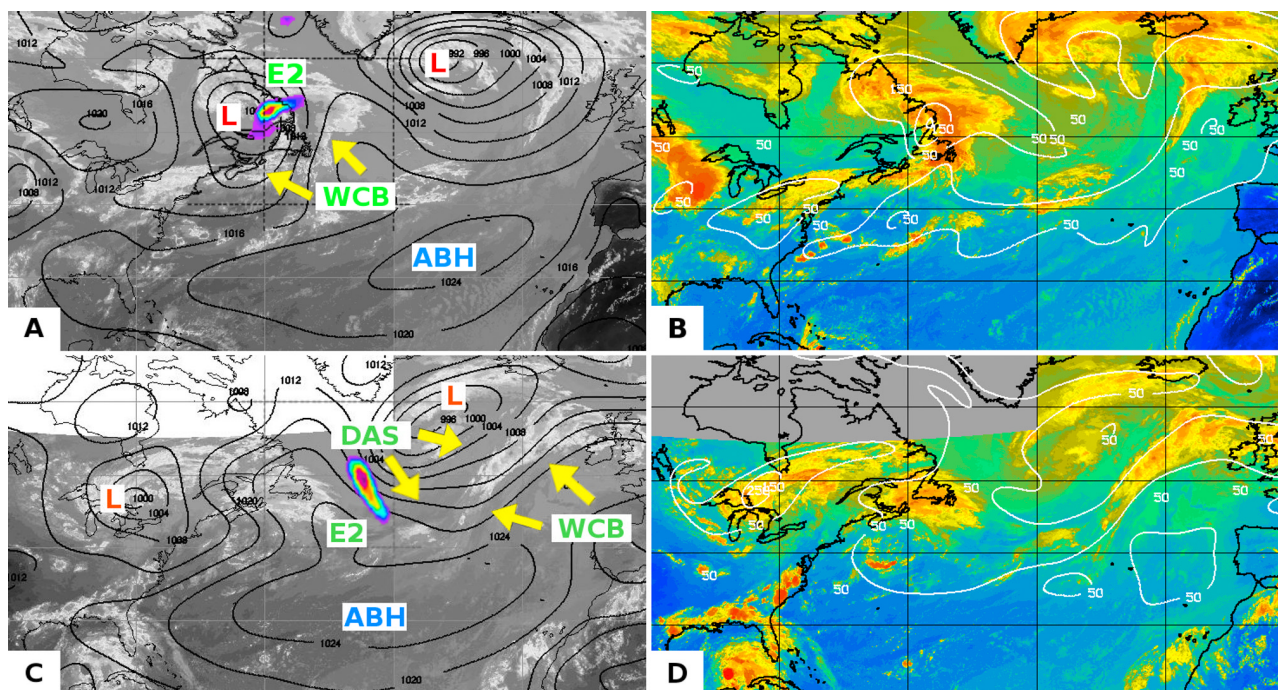


**Figure 5.** The 24-hour average location of the retroplume for event 2, plotted on top of combined GOES-EAST and METEOSAT infrared image and sea level isobars (left column) and 4–20 km CO column isolines (right column) plotted on top of the same infrared image shown in false color. The retroplume shown in the left column was initialized during event 2 (1200–1500 UTC 13 July). Times shown are (a and b) 1200 UTC on 9 July and (c and d) 0000 UTC on 12 July. Labels on the left-hand plots indicate the retroplume for event 2 (E2) and pertinent meteorological features (low pressure centers, L; associated warm conveyor belts, WCB; dry airstreams, DAS; and the Azores-Bermuda High, ABH).

American CO during this event, shown in Figure 4c, included contributions from a rather large region of the northern United States and southern Canada, with particularly strong signals from Boston, Toronto, Detroit, and Chicago. The retroplume originated over this region on 9 July, 4.5 days before arriving at the PICO-NARE station.

### 3.2.1. Export Out of the U.S. Boundary Layer in the Westerly Wind

[34] The features of this event are distinctly different from those of event 1, beginning with the meteorological scenario that led to the export. On 7 July at 0000 UTC (–6 days) a low-pressure system was located over southern Manitoba and Ontario. Unlike the case prior to event 1, however, a high-pressure system was not present and the eastern United States did not experience dampened export. Instead, pollution was being actively exported out of the U.S. boundary layer. Figures 3e and 3f, discussed above in the context of event 1, show continuing CO export on 7 July, with a CO plume being channeled out of the United States between the ABH and the low responsible for the transport of event 1, located over the northwestern Atlantic at this time.

[35] The next day, the Canadian low tracked east, and by 0000 UTC on 8 July (–5 days), it was located over northern Quebec and Newfoundland. At this time the low, in conjunction with the ABH, was still zonally channeling CO into the Atlantic. Later on 8 July, a region of high pressure began to form between the Canadian and Atlantic lows. This region of high pressure, coupled with the intensification of the Canadian low, shifted most of the low-level flow of CO to

the north-northeast, toward the center of the low, early on 9 July (–4.5 days, shortly before the time shown in Figure 5a). By this time, the low was over northeastern Quebec and Newfoundland. As a result, the most intense portion of the CO plume had moved northeast from its source over the Mid-Atlantic states and southern New England. At 0000 UTC on 9 July, part of the plume was located over northern Maine and Nova Scotia. The larger portion was over the western Atlantic, off the east coast of Maine, distributed from the surface up to about 3 km, with the bulk in the lower kilometer.

### 3.2.2. Rapid Lofting and Subsidence

[36] Shortly after the shift in the flow regime, the cold front associated with the Canadian low passed over the northeastern United States, southeastern Canada, and the adjacent portion of the Atlantic, including a large section of the CO plume. As a result, the CO plume was lofted in the warm conveyor belt ahead of the front. This frontal passage began at approximately 0000 UTC on 9 July (–4.5 to –4 days). The location of the retroplume at 1200 UTC on 9 July, shortly after the cold front's passage, is shown in Figure 5a. Figure 5b shows the 4–20 km CO column calculated by the forward FLEXPART simulation at this time; the lofted CO plume is apparent near the center of the comma cloud associated with the WCB uplift. (In contrast, Figure 3h shows much less CO present in the 0–3 km column at the retroplume's location at this time.)

[37] Over the next 3 days, the Canadian low continued to track eastward, with the pressure center moving over the

Atlantic early on 10 July (−3 days). Around 12 July (−1.5 days), the low began to weaken and track northeastward. During this time, the cold front continued to sweep eastward, eroding the warm sector.

[38] During the cyclone's trek over the Atlantic, the retroplume of North American CO emissions destined to reach the PICO-NARE station also tracked eastward, traveling cyclonically around the center of the pressure system from the eastern side on 9 July (−4 days), to the northern side on 10 July (−3 days), and finally to the western side on 11 July (−2 days). The plume continued to rise during 9 and 10 July, reaching a maximum height of approximately 6.5 km at 0000 UTC on 11 July (−2.5 days). After arriving on the western side of the low, the retroplume became entrained in the cold descending air behind the cold front (the dry airstream [Cooper *et al.*, 2001]). Once this happened, the retroplume rapidly descended toward the southeast, and by 0000 UTC on 12 July (−1.5 days) it was traveling rapidly toward the Azores (Figure 5c). It arrived at the station on 13 July, immediately behind the cold front.

[39] In summary, the events that led to the elevated CO and O<sub>3</sub> levels observed over the Azores during this event began with the low-level export of emissions from the U.S. boundary layer in westerly winds. This was followed by the lofting of the pollution to 6–8 km altitude in the warm conveyor belt ahead of the cold front associated with a passing northerly cyclone. However, despite being lofted to high altitude, the plume was observed at 2.2 km over the Azores, as a result of incorporation into the same cyclone's descending dry air stream. A similar process was observed by Cooper *et al.* [2001] over the western North Atlantic Ocean, but was not observed to descend as strongly as in the present case study.

### 3.3. Events 3 and 4: Export in a Weak Warm Conveyor Belt Followed by Transport Around the Azores High

[40] Two additional episodes of elevated CO were observed at the station in the period of 20–22 July 2003. The first (event 3) arrived during 0000–0400 UTC 20 July and the second (event 4) arrived during 0600–1300 UTC 22 July. Though these events arrived 2 days apart, they were exported out of the U.S. boundary layer in the same frontal system and had similar transport pathways until 18 July, when their paths diverged.

[41] Using FLEXPART retroplumes initiated during 0000–0300 UTC 20 July for event 3, and 1200–1500 UTC 22 July for event 4, the retroplumes can be traced back to the U.S. east coast, where the bulk of the CO originated over New England and the Mid-Atlantic states on 15 July (−5 days and −7 days for events 3 and 4, respectively). The two events are described together here because they were exported at the same time and the subsequent transport is closely linked.

[42] Column-integrated retroplume residence times are shown for both events in Figures 6a and 6b. Their general features are very similar, though event 3 (Figure 6a) exhibits a greater degree of dispersion. The footprint layer residence times (Figures 6c and 6d) indicate that most time spent in the footprint layer was over the eastern and midwestern United States for both plumes, though the plume for event 4 (Figure 6d) also spent time in the marine boundary layer south of the Azores. Figures 6e and 6f show broad CO

contributions from the eastern United States, with the Boston area being particularly important for event 3.

#### 3.3.1. Export Out of the U.S. Boundary Layer in a Weak Warm Conveyor Belt

[43] On 15 July, there were two meteorological features that contributed to the export responsible for these events: a region of high pressure over the eastern United States and a weak low-pressure system over Canada, north of Lake Superior. The high dampened convection over the northeastern United States and reduced the export of pollution out of the U.S. boundary layer, as was also the case prior to event 1. The low will be responsible for the export that resulted in this event.

[44] During 15 July the low strengthened, and a cold front formed and began to move southeast. The low tracked east-southeast, with the center of the low passing over southeastern Ontario and southern Quebec on 16 July. Meanwhile, the high-pressure system retreated eastward as the low pushed into the region (Figure 7a). The cold front continued to move southeast around the low-pressure center, reaching the U.S. east coast around 1200 UTC on 16 July. As the front passed over the region, the CO plume was exported out of the U.S. boundary layer in a warm conveyor belt, which was visible as a thin line of clouds that extended from the midwestern United States to the northeastern U.S. coast (Figures 7a and 7b). The export height, however, was limited to the lower free troposphere because of the relatively weak intensity of the low-pressure system and the small temperature difference across the front. This is indicated in the FLEXPART forward results, which include the majority of the plume within the lower 3 km of the atmosphere. For this reason, 0–3 km CO columns are shown in Figures 7b, 7d, and 7f.

[45] The daily averaged retroplumes for each event (Figure 7a) indicate only slight differences in location during the export phase on 16 July, despite their arrival time at the Azores 2 days apart. However, the export of retroplume particles arriving during event 4 occurred a few hours later and farther south than that for event 3.

#### 3.3.2. Transport to the Station in Gradient Winds

[46] By 1200 UTC on 17 July, the cold front had dissipated, and the low-pressure system had merged with a second low, creating a large region of low pressure over northeastern Canada. At this time the ABH was located over the central North Atlantic, centered roughly midway between the Azores and the North American east coast. The formation of the larger low-pressure region caused the northeastern edge of the ABH to retreat, leaving the CO plume located between the two pressure systems, with the portion of the plume for event 3 closer to the ABH and the portion of the plume for event 4 closer to the low.

[47] During the next day, the main CO plume tracked northeast, as it was channeled by the resulting gradient wind. By 18 July, the two retroplumes had diverged significantly, as the event 3 retroplume had traveled primarily east because of its proximity to the ABH, while the event 4 retroplume had traveled northeast, because of its proximity to the Canadian low (Figures 7c and 7d).

[48] As the event 3 retroplume moved east of the influence of the ABH and the Canadian low, it encountered another low-pressure system located northeast of the Azores. As a result, on 18 and 19 July, the event 3 retroplume

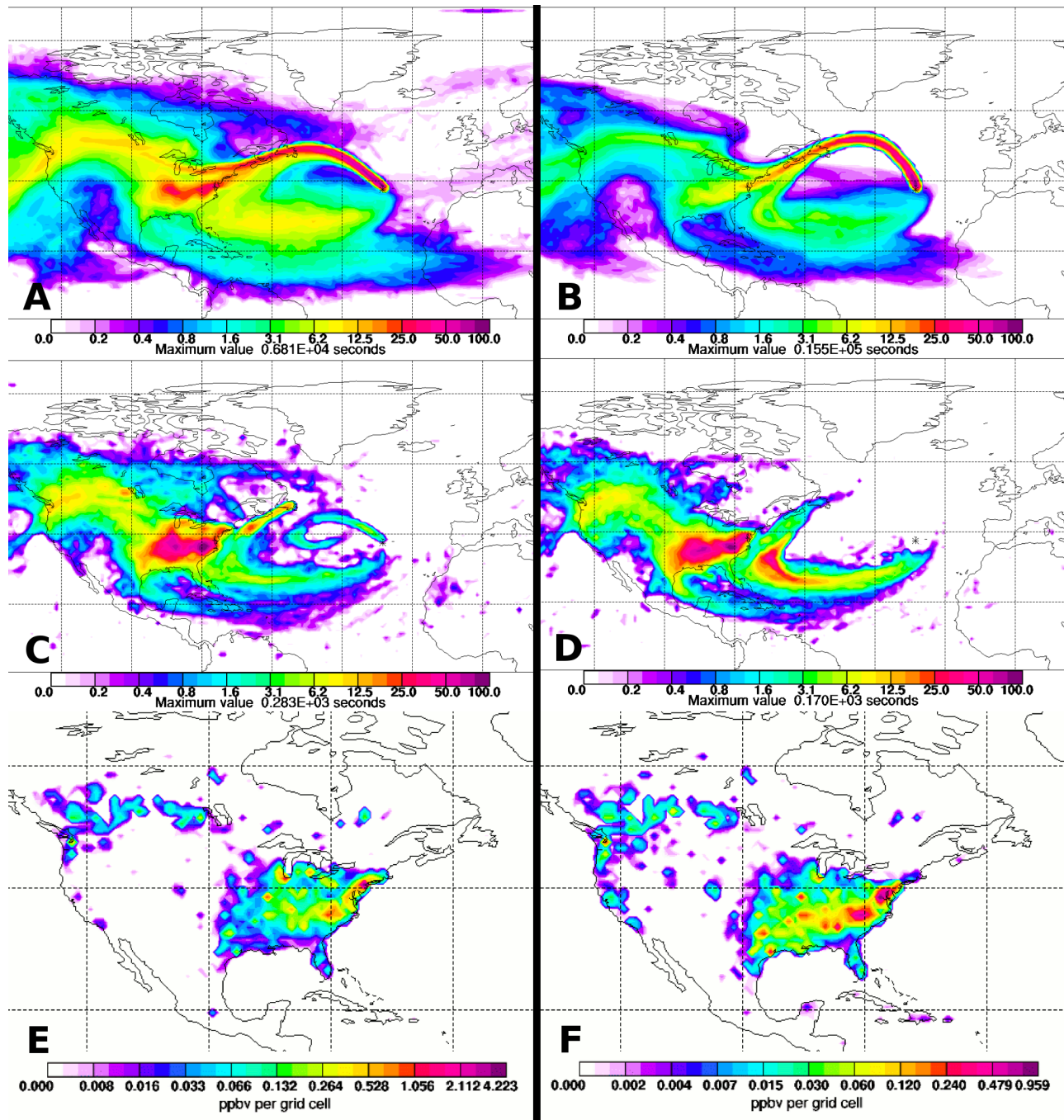


**Figure 6.** FLEXPART retroplume results for events 3 (left column) and 4 (right column). (a) Column integrated residence time for event 3, (b) column integrated residence time for event 4, (c) residence time in the 0–300 m footprint layer for event 3, (d) residence time in the 0–300 m footprint layer for event 4, (e) source contributions to CO mixing ratio calculated during event 3, and (f) source contributions to CO mixing ratio calculated during event 4. The retroplume for event 3 was initiated 0000–0030 UTC 20 July; that for event 4 was initiated 0000–0300 UTC 22 July.

traveled southeast toward the Azores in the gradient wind between the ABH and the Atlantic low (Figures 7c and 7e). Meanwhile, the event 4 retroplume continued to travel northeast until approximately 0000 UTC 19 July, when the Atlantic low began to influence its transport (about 1.5 days later than for event 3), and when it began to track southeast toward the Azores (Figure 7e).

[49] Over the next day, both plumes continued to track southeast toward the station, with event 3 arriving on 20 July. The transport of the event 4 retroplume was slowed, however, by the retreat of the Atlantic low to the northeast, which left the plume in a weaker gradient wind closer to the center of the ABH. By 21 July, the low had advanced far enough to the northeast that the plume was no longer being

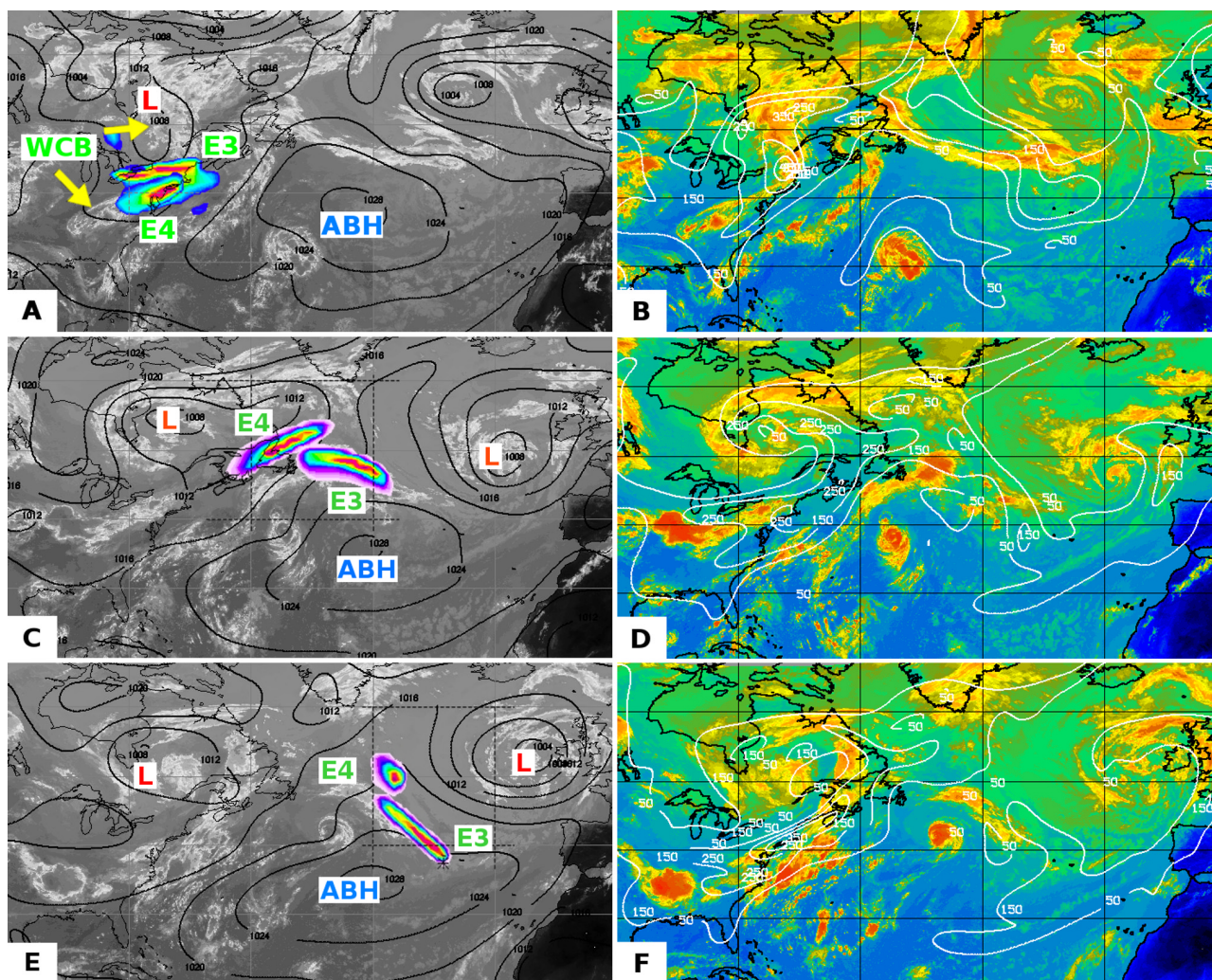


**Figure 7.** The 24-hour average locations of the retroplumes for events 3 and 4, plotted on top of combined GOES-EAST and METEOSAT infrared image and sea level isobars (left column) and 0–3 km CO column isolines (right column) plotted on top of the same infrared image shown in false color. The retroplumes shown in the left column were initialized during event 3 (0000–0300 UTC 20 July) and event 4 (0000–0300 UTC 22 July). Times shown are (a and b) 1200 UTC on 16 July, (c and d) 1200 UTC on 18 July, and (e and f) 1200 UTC on 19 July. Labels on the left-hand plots indicate the retroplume for events 3 and 4 (E3 and E4) and pertinent meteorological features (low pressure centers, L; associated warm conveyor belts, WCB; and the Azores-Bermuda High, ABH).

channeled between the pressure features. Instead, it was on the eastern edge of the ABH where it experienced significantly reduced transport speeds during its last day of travel, before arriving at the station on 22 July.

[50] In summary, the elevated CO and O<sub>3</sub> levels observed over the Azores during these events were the result of the accumulation of emissions under a stagnant high-pressure system, followed by weak lofting to the lower free troposphere in a weak warm conveyor belt associated with a low passing to the north. The emissions were then transported to the Azores in gradient winds governed by the relative location of a Canadian low, an Atlantic low, and the ABH. This pair of events has the interesting attribute of being exported as essentially one plume, while arriving separated by 2 days. This was the result of initially small location differences that were amplified as the plumes were advected

by the gradient winds between the ABH and two evolving lows to the north.

#### 4. Discussion

[51] The four events analyzed here are typical of those reaching the central North Atlantic lower FT during the summertime, as indicated by observations at the PICONARE station and summarized in Table 1. Transport in the lower troposphere was responsible for the majority of these events: the FLEXPART forward simulations indicate that transport of North American CO emissions to the Azores occurred primarily below 3 km in three of the four events analyzed in detail (events 1, 3, and 4), and in a total of 13 of the 16 events (84% of the total event hours) in Table 1. Significant O<sub>3</sub> enhancements were also observed in

most of these events (Table 1) and in additional similar events in 2001 and 2003 that we analyzed previously [Honrath *et al.*, 2004]. The previous analysis was based on backward trajectories, and identified North American emissions as a significant contributor to the events analyzed here; the present work confirms this. The previous analysis also identified biomass burning as a possible contributor to the CO enhancements observed in many of these events, though not in event 4 analyzed above. The analysis presented here is not affected by the likely presence of an admixture of biomass-burning emissions.

[52] We now briefly discuss the relevance of these low-level events to North American pollution export and downwind impacts.

[53] The altitude dependence of CO export from North America has been calculated by *Li et al.* [2005], Table 1 using GEOS-CHEM simulations for July of 4 years. On average, 38% of the total North American CO export (eastward across 70°N) occurs below 3 km altitude. Thus the low-level events discussed above are not unusual. Events of this type also impact CO mixing ratios at low levels over Europe. For example, results from a 1-year FLEXPART simulation of the transport of North American CO emissions indicate that peak impacts over Europe (at 5°E) of CO emissions emitted 10–12 days earlier occur below 3 km altitude (though significant North American CO is present from the surface to 7 km) [Stohl *et al.*, 2002a].

[54] The relevance of low-level transport events to O<sub>3</sub> mixing ratios and fluxes over Europe has been addressed in several recent studies using the GEOS-CHEM model. *Auvray and Bey* [2005] and *Li et al.* [2002] both analyzed the impact of North American emissions on fluxes O<sub>3</sub> and resulting surface mixing ratios over Europe. *Auvray and Bey* [2005] found that horizontal advection through the boundary layer (defined as the region below 600 hP) accounted for approximately one third of the total summertime flux of O<sub>3</sub> produced from North American emissions into the European boundary layer for 1997, contributing approximately an additional 2.7 ppb of O<sub>3</sub> [Auvray and Bey, 2005, Figures 13 and 15]. *Li et al.* [2002] analyzed a 5-year (1993–1997) simulation and found that low-level (less than 3-km altitude) transport contributed significantly to North American impacts on European surface O<sub>3</sub> mixing ratios. On average, they found that during the summer, North American sources contributed 2–4 ppb of O<sub>3</sub> and 5–10 ppb during transport events, with low-level flux into the boundary layer being as important as subsidence into the boundary layer. The events responsible for the largest enhancements of North American O<sub>3</sub> at European surface sites were the result of low-level westerly flow under conditions typified by a strong Icelandic Low located between Iceland and the British Isles. This situation is identical to that present in Figures 3g and 3h, which show the continued advection toward Europe of the northern portion of the large CO plume responsible for event 1. Several specific low-level events of this type are discussed by *Guerova et al.* [2005], who compare the resulting GEOS-CHEM-simulated O<sub>3</sub> enhancements over Europe to observations.

[55] However, it has been noted that North American pollution is rarely seen at European surface sites [e.g., *Derwent et al.*, 1998]. *Stohl et al.* [2002a] identified two possible reasons for this. Firstly, North American pollution

reaches the European surface primarily south of the Pyrenees, where measurements sites are sparse, and secondly, the age of these plumes are generally older (more than 10 days old) and therefore hard to accurately trace back to sources on a case study basis. Additionally, North American emissions may also recirculate, turning anticyclonically around the ABH and head back toward the continent [Auvray and Bey, 2005]. This was fate of 14 of the 16 events in Table 1 based on HYSPLIT trajectories [Draxler and Rolph, 2003; Rolph, 2003] initiated at the station during each event; only events b and h head toward Europe, reaching the UK after 3 days and Spain after 3.5 days, respectively. The Azores, however, are located slightly south of the low-level flow path that more often leads to Europe [e.g., Auvray and Bey, 2005, Figure 7] and so our results do not necessarily reflect the percentage of North American air that is transported in the lower troposphere, reaching Europe.

[56] Many previous studies have also emphasized that long-range transport of O<sub>3</sub> exported into the MBL is unlikely and rarely observed because of the short O<sub>3</sub> lifetime in the MBL [e.g., *Derwent et al.*, 1998; *Jaffe et al.*, 2003; *Price et al.*, 2004; *Auvray and Bey*, 2005]. However, the low-level export events discussed here (events 1, 3, and 4) were exported below 3 km altitude, but significant O<sub>3</sub> enhancements were observed in events 3 and 4 (O<sub>3</sub> measurements are unavailable for event 1). Similar events in 2001 also produced characteristically significant O<sub>3</sub> increases [Honrath *et al.*, 2004]. However, the O<sub>3</sub> enhancements in both years were observed in the marine FT, not the MBL. This underscores the fact that BL structure over the oceans differs significantly from that over land, with the result that portions of plumes exported at low altitudes can be incorporated into the marine lower FT. Near the coast, exported continental plumes produce pollutant layers in a statically stable atmosphere with weak vertical mixing [Angevine *et al.*, 2004]. Over time, as the continental air mass travels over the ocean, an internal boundary layer develops [Skylingstad *et al.*, 2005], ultimately becoming a steady state mixed layer [Smedman *et al.*, 1997], i.e., the MBL, and leaving a portion of the exported plume in what is now the lower FT. Alternatively, weak uplift as described for events 3 and 4 may loft the pollution directly into the lower FT. Lower FT transport of this type provides a mechanism for the long-range transport of continental pollution without the dehydration, dilution, scavenging, and expansion generally associated with uplift to high altitudes, yet also without the greatly enhanced loss rates present in the MBL.

[57] Finally, the importance of low-level transport to the Azores and the lower FT of the Central North Atlantic is a significant result. Midlatitude cyclones are responsible for most of the pollution outflow from North America to the North Atlantic as they track eastward across the United States [Merrill and Moody, 1996; *Li et al.*, 2005]. Specifically, WCB transport is a primary mechanism for the export of polluted air from the continental boundary layer and subsequent intercontinental transport [Cooper and Parrish, 2004]. However, only 2 events (event 2 of the case studies and event 1 from Table 1) out of 16 observed at the PICONARE station experienced lofting to the middle troposphere that is typical of WCB events responsible for intercontinental pollution transport. This analysis indicates that WCBs

are not dominant mechanisms for transport to the Central North Atlantic lower FT during summer. Instead, advection of pollution layers at low levels, but decoupled from the MBL is responsible for the majority of transport into the region during summertime.

## 5. Summary and Conclusions

[58] We have used the Lagrangian particle dispersion model FLEXPART to simulate the transport of North American CO emissions to the PICO-NARE station in the central North Atlantic lower free troposphere during July 2003. FLEXPART adequately captured the occurrence of CO transport events: North American anthropogenic CO enhancements of at least 10 ppbv were simulated during 15 of 16 events of enhanced CO actually observed, but only in three events not apparent in the observations. These observed events were quite frequent during July 2003, occurring on 68% of the days for which CO measurements are available. The evolving meteorological situations responsible for four of these events were analyzed in detail.

[59] Two mechanisms were responsible for the export of pollution from the North American boundary layer that led to these events: direct advection from the continental boundary layer eastward over the Atlantic Ocean, and uplift ahead of cold fronts. In most simulated events, export occurred at low altitudes (below  $\sim 3$  km). Three case studies of low-level events were presented, including two events exported in the same weak warm conveyor belt event. In these three cases, and in a majority of all the events simulated by FLEXPART, the subsequent transport to the Azores occurred in the lower troposphere and was the result of flow channeled between the Azores/Bermuda High and one or more lows passing to the north. The pathway followed by the pollutant plumes in these events is therefore sensitive to the location of these features, and situations only moderately different than those analyzed here can result in similar events reaching Europe.

[60] Although the result of low-level export, these events were nevertheless observed in the free troposphere over the Azores, and O<sub>3</sub> enhancements were observed coincident with CO in most cases. Since low-level export of North American emissions accounts for a significant portion of the total summertime CO export [Li *et al.*, 2005], we suggest that low-level continental export leading to transport in the lower troposphere, but above the marine boundary layer, may provide an effective mechanism for long-range impacts of anthropogenic emissions on lower tropospheric O<sub>3</sub> in downwind regions.

[61] A fourth event described in detail was the result of uplift to above 6 km in the warm conveyor belt associated with a cyclone passing to the north. The emissions that reached the Azores were captured in the midtropospheric circulation around the center of the low for 2 days, before becoming entrained in the same cyclone's dry airstream. The event was observed when the dry airstream reached the Azores following the passage of the front 1 day later.

[62] **Acknowledgments.** We would like to thank Mike Dziobak and María Val Martín for their continuous efforts in helping to maintain and run the station and Sabine Eckhardt and Nicole Spichtinger for retrieving the ECMWF data used in this work. In addition, we gratefully acknowledge the assistance of Paul Novelli and Sam Oltmans (NOAA CMDL) with the

referencing of our measurements to CMDL and NIST standards. This work was supported by NOAA, Office of Global Programs, grants NA16GP1658, NA86GP0325 and NA03OAR4310002, and the National Science Foundation, grant INT-0110397. The GOES-EAST images and AVN analyses were made available through the UNIDATA McIDAS data stream and displayed using UNIDATA McIDAS software. METEOSAT images were provided by the Space Science and Engineering Center, University of Wisconsin-Madison. The authors gratefully acknowledge the NOAA Air Resources Laboratory (ARL) for the provision of the HYSPLIT transport and dispersion model and/or READY website (<http://www.arl.noaa.gov/ready.html>) used in this publication.

## References

- Angevine, W. M., et al. (2004), Coastal boundary layer influence on pollutant transport in New England, *J. Appl. Meteorol.*, *43*, 1425–1437.
- Auvray, M., and I. Bey (2005), Long-range transport to Europe: Seasonal variations and implications for the European ozone budget, *J. Geophys. Res.*, *110*, D11303, doi:10.1029/2004JD005503.
- Cooper, O., and D. Parrish (2004), Air pollution export from and import to North America: Experimental evidence, in *The Handbook of Environmental Chemistry*, vol. 4G, pp. 41–67, edited by A. Stohl, Springer, New York.
- Cooper, O., et al. (2001), Trace gas signatures of the airstreams within North Atlantic cyclones: Case studies from the North American Regional Experiment (NARE '97) aircraft intensive, *J. Geophys. Res.*, *106*, 5437–5456.
- Cooper, O. R., J. L. Moody, D. D. Parrish, M. Trainer, T. B. Ryerson, J. S. Holloway, G. Hbler, F. C. Fehsenfeld, and M. J. Evans (2002), Trace gas composition of midlatitude cyclones over the western North Atlantic Ocean: A conceptual model, *J. Geophys. Res.*, *107*(D7), 4056, doi:10.1029/2001JD000901.
- Cooper, O. R., et al. (2004), A case study of transpacific warm conveyor belt transport: Influence of merging airstreams on trace gas import to North America, *J. Geophys. Res.*, *109*, D23S08, doi:10.1029/2003JD003624.
- Derwent, R., P. Simmonds, S. Seuring, and C. Dimmer (1998), Observations and interpretation of the seasonal cycles in the surface concentrations of ozone and carbon monoxide at Mace Head, Ireland from 1990 to 1994, *Atmos. Environ.*, *32*, 145–157.
- Dickerson, R. R., et al. (1987), Thunderstorms: An important mechanism in the transport of air pollutants, *Science*, *235*, 460–465.
- Draxler, R. R., and G. D. Rolph (2003), HYSPLIT (Hybrid Single-Particle Lagrangian Integrated Trajectory), Model access via NOAA ARL READY website, NOAA Air Resour. Lab., Silver Spring, Md. (Available at <http://www.arl.noaa.gov/ready/hysplit4.html>)
- European Center for Medium-Range Weather Forecasts (1995), Users guide to ECMWF products 2.1, *Tech. Rep. Meteorol. Bull. M3.2*, Reading, U. K.
- Guerova, G., I. Bey, L.-L. Attie, and R. Martin (2005), Case studies of ozone transport between North America and Europe in summer 2000, *Atmos. Chem. Phys. Disc.*, *5*, 6127–6148.
- Hoell, J., D. Davis, S. Liu, R. Newell, H. Akimoto, R. McNeal, and R. Bendura (1997), The Pacific Exploratory Mission—West Phase B: February–March, 1994, *J. Geophys. Res.*, *102*, 28,223–28,239.
- Honrath, R., R. Owen, M. V. Martin, J. Reid, K. Lapina, P. Fialho, M. Dzoibak, J. Kleissl, and D. Westphal (2004), Regional and hemispheric impacts of anthropogenic and biomass burning emissions on summertime CO and O<sub>3</sub> in the North Atlantic lower free troposphere, *J. Geophys. Res.*, *109*, D24310, doi:10.1029/2004JD005147.
- Houghton, J. T., Y. Ding, D. J. Griggs, M. Noguer, P. J. van der Linden, X. Dai, K. Maskell, and C. A. Johnson (Eds.) (2001), *Climate Change 2001: The Scientific Basis—Contribution of Working Group I to the Third Assessment Report of the Intergovernmental Panel on Climate Change*, Cambridge Univ. Press, New York.
- Huntrieser, H., et al. (2005), Intercontinental air pollution transport from North America to Europe: Experimental evidence from airborne measurements and surface observations, *J. Geophys. Res.*, *110*, D01305, doi:10.1029/2004JD005045.
- Jaffe, D., et al. (1999), Transport of Asian air pollution to North America, *Geophys. Res. Lett.*, *26*, 711–714.
- Jaffe, D., I. McKendry, T. Anderson, and H. Price (2003), Six “new” episodes of trans-Pacific transport of air pollutants, *Atmos. Environ.*, *37*, 391–404.
- Li, Q., et al. (2002), Transatlantic transport of pollution and its effects on surface ozone in Europe and North America, *J. Geophys. Res.*, *107*(D13), 4166, doi:10.1029/2001JD001422.
- Li, Q., D. J. Jacob, R. Park, Y. Wang, C. L. Heald, R. Hudman, R. M. Yantosca, R. V. Martin, and M. Evans (2005), North American pollution outflow and the trapping of convectively lifted pollution by upper-level anticyclone, *J. Geophys. Res.*, *110*, D10301, doi:10.1029/2004JD005039.

- Merrill, J. T., and J. L. Moody (1996), Synoptic meteorology and transport during the North Atlantic Regional Experiment (NARE) intensive: Overview, *J. Geophys. Res.*, *101*, 28,903–28,921.
- Neuman, A., et al. (2006), Reactive nitrogen transport and photochemistry in urban plumes over the North Atlantic Ocean, *J. Geophys. Res.*, *111*, D23S54, doi:10.1029/2005JD007010.
- Olivier, J., and J. Berdowski (2001), Global emissions sources and sinks, in *The Climate System*, edited by J. Berdowski, R. R. Guicherit, and B. Heij, pp. 33–78, A. A. Balkema, Brookfield, Vt.
- Park, R. J., D. J. Jacob, B. D. Field, R. M. Yantosca, and M. Chin (2004), Natural and transboundary pollution influences on sulfate-nitrate-ammonium aerosols in the United States: Implications for policy, *J. Geophys. Res.*, *109*, D15204, doi:10.1029/2003JD004473.
- Parrish, D., M. Trainer, J. Holloway, J. Yee, M. Warshawsky, and F. Fehsenfeld (1998), Relationships between ozone and carbon monoxide at surface sites in the North Atlantic region, *J. Geophys. Res.*, *103*, 13,357–13,376.
- Parrish, D. D., M. Trainer, D. Hereid, E. J. Williams, K. J. Olszyna, R. A. Harley, J. F. Meagher, and F. C. Fehsenfeld (2002), Decadal change in carbon monoxide to nitrogen oxide ratio in U.S. vehicular emissions, *J. Geophys. Res.*, *107*(D12), 4140, doi:10.1029/2001JD000720.
- Pickering, K. E., A. M. Thompson, R. R. Dickerson, W. T. Luke, D. P. McNamara, J. P. Greenberge, and P. R. Zimmerman (1990), Model calculations of tropospheric ozone production potential following observed convective events, *J. Geophys. Res.*, *95*, 14,049–14,062.
- Pochanart, P., H. Akimoto, Y. Kajii, V. M. Potemkin, and T. V. Khodzher (2003), Regional background ozone and carbon monoxide variations in remote Siberia/East Asia, *J. Geophys. Res.*, *108*(D1), 4028, doi:10.1029/2001JD001412.
- Price, H. U., D. A. Jaffe, O. R. Cooper, and P. V. Doskey (2004), Photochemistry, ozone production, and dilution during long-range transport episodes from Eurasia to the northwest United States, *J. Geophys. Res.*, *109*, D23S13, doi:10.1029/2003JD004400.
- Rodrigues, S., C. Torres, J.-C. Guerra, and E. Cuevas (2004), Transport pathways of ozone to marine and free-troposphere sites in Tenerife, Canary Islands, *Atmos. Environ.*, *38*, 4733–4747.
- Rolph, G. D. (2003), Real-time Environmental Applications and Display sYstem (READY) website, NOAA Air Resour. Lab., Silver Spring, Md. (Available at <http://www.arl.noaa.gov/ready/hysplit4.html>)
- Ryall, D. B., R. H. Maryon, R. G. Derwent, and P. G. Simmonds (1998), Modelling long-range transport of CFCs to Mace Head, Ireland, *Q. J. R. Meteorol. Soc.*, *124*, 417–446.
- Seibert, P., and A. Frank (2004), Source-receptor matrix calculation with a Lagrangian particle dispersion model in backward mode, *Atmos. Chem. Phys.*, *4*, 51–63.
- Skyllingstad, E. D., R. M. Samelson, L. Mahrt, and P. Barbour (2005), A numerical modeling study of warm offshore flow over cool water, *Mon. Weather Rev.*, *133*, 345–361.
- Smedman, A.-S., H. Bergström, and B. Grisogono (1997), Evolution of stable internal boundary layers over a cold sea, *J. Geophys. Res.*, *102*, 1091–1099.
- Stohl, A., and D. J. Thomson (1999), A density correction for Lagrangian particle dispersion models, *Boundary Layer Meteorol.*, *90*, 155–167.
- Stohl, A., and T. Trickl (1999), A textbook example of long-range transport: Simultaneous observation of ozone maxima of stratospheric and North American origin in the free troposphere over Europe, *J. Geophys. Res.*, *104*, 30,445–30,462.
- Stohl, A., and T. Trickl (2001), Experimental evidence for trans-Atlantic transport of air pollution, *IGACTivities Newsl.*, *24*, 10–12.
- Stohl, A., M. Hittenberger, and G. Wotawa (1998), Validation of the Lagrangian particle dispersion model FLEXPART against large scale tracer experiment data, *Atmos. Environ.*, *24*, 4245–4264.
- Stohl, A., S. Eckhardt, C. Forster, P. James, and N. Spichtinger (2002a), On the pathways and timescales of intercontinental air pollution transport, *J. Geophys. Res.*, *107*(D23), 4684, doi:10.1029/2001JD001396.
- Stohl, A., M. Trainer, T. B. Ryerson, J. S. Holloway, and D. D. Parrish (2002b), Export of NO<sub>y</sub> from the North American boundary layer during 1996 and 1997 North Atlantic Regional Experiments, *J. Geophys. Res.*, *107*(D11), 4131, doi:10.1029/2001JD000519.
- Stohl, A., C. Forster, S. Eckhardt, N. Spichtinger, H. Huntrieser, J. Heland, H. Schlager, S. Wilhelm, F. Arnold, and O. Cooper (2003), A backward modeling study of intercontinental pollution transport using aircraft measurements, *J. Geophys. Res.*, *108*(D12), 4370, doi:10.1029/2002JD002862.
- Stohl, A., O. Cooper, and P. James (2004), A cautionary note on the use of meteorological analysis fields for quantifying atmospheric mixing, *J. Atmos. Sci.*, *61*, 1446–1453.
- Thompson, A. M., K. E. Pickering, R. R. Dickerson, W. G. Ellis Jr., D. J. Jacob, J. R. Scala, W. Tao, D. P. McNamara, and J. Simpson (1994), Convective transport over the central United States and its role in regional CO and ozone budgets, *J. Geophys. Res.*, *99*(D9), 18,703–18,712.
- Trickl, T., O. R. Cooper, H. Eisele, P. James, R. Mcke, and A. Stohl (2003), Intercontinental transport and its influence on the ozone concentrations over central Europe: Three case studies, *J. Geophys. Res.*, *108*(D12), 8530, doi:10.1029/2002JD002735.

O. R. Cooper, Cooperative Institute for Research in Environmental Sciences, University of Colorado/NOAA Earth System Research Laboratory, Boulder, CO 80309, USA.

R. E. Honrath and R. C. Owen, Department of Civil and Environmental Engineering, Michigan Technological University, Houghton, MI 49931-1295, USA.

A. Stohl, Norwegian Institute for Air Research, Instituttueien 18, P.O. Box 100, N-2027 Kjeller, Norway.